PHILOSOPHICAL TRANSACTIONS OF THE ROYAL SOCIETY B BIOLOGICAL SCIENCES

Design strategies of sea urchin teeth: structure, composition and micromechanical relations to function

R. Z. Wang, L. Addadi and S. Weiner

Phil. Trans. R. Soc. Lond. B 1997 **352**, 469-480
doi: 10.1098/rstb.1997.0034

Design strategies of sea urchin teeth: structure, composition and micromechanical relations to function

R. Z. WANG, L. ADDADI AND S. WEINER*

Department of Structural Biology, Weizmann Institute of Science, Rehovot 76100, Israel

SUMMARY

The teeth of sea urchins comprise a variety of different structural entities, all of which are composed of magnesium-bearing calcite together with a small amount of organic material. The teeth are worn down continuously, but in such a way that they remain sharp and functional. Here we describe aspects of the structural, compositional and micromechanical properties of the teeth of *Paracentrotus lividus* using scanning electron microscopy, infrared spectrometry, atomic absorption, X-ray diffraction and microindentation. The S-shaped single crystalline calcitic fibres are one of the main structural elements of the tooth. They extend from the stone part to the keel. The diameter of the fibres increases gradually from less than 1 μm at the stone tip to about 20 μm at the keel end, while their $MgCO_3$ contents decrease from about 13 mol% to about 4.5 mol%. Each fibre is coated by a thin organic sheath and surrounded by polycrystalline calcitic discs containing as much as 35 mol% $MgCO_3$. This structure constitutes a unique kind of gradient fibre-reinforced ceramic matrix composite, whose microhardness and toughness decrease gradually from the stone part to the keel. Primary plates are also important structural elements of the tooth. Each primary plate has a very unusual sandwich-like structure with a calcitic envelope surrounding a thin apparently amorphous $CaCO_3$ layer. This central layer, together with the primary plate/disc interface, improves the toughness of this zone by stopping and blunting cracks. The self-sharpening function of the teeth is believed to result from the combination of the geometrical shape of the main structural elements and their spatial arrangement, the interfacial strength between structural elements, and the hardness gradient extending from the working stone part to the surrounding zones. The sea urchin tooth structure possesses an array of interesting functional design features, some of which may possibly be applicable to materials science.

1. INTRODUCTION

Biogenic composite materials, such as bones, teeth, mollusc shells, etc., are well recognized for their complex structures and outstanding mechanical properties (Weiner 1986; Lowenstam & Weiner 1989; Mann *et al.* 1989; Vincent 1990; Addadi & Weiner 1992; Heuer *et al.* 1992). The functions of teeth are generally better understood compared to other biologically produced materials. The study of their design strategies in terms of structure–function relations, therefore, offers many advantages. The teeth of the echinoids or sea urchins are of particular interest. They are composed almost entirely of $CaCO_3$, mainly in the form of magnesium-bearing calcite. The shape, size and compositions of the crystals are diverse and the resulting structure is very complex (Märkel 1970; Märkel *et al.* 1977). In this study we address not only the manner in which the structures are adapted to function, but also elaborate on the interesting observation that the mineral phase itself is fine-tuned to functional use.

The echinoids are marine invertebrates belonging to the phylum Echinodermata. Many echinoids have five elongated and slightly curved teeth, each of which has the same morphology and structure (Hyman 1955; Barnes 1987). The five teeth are part of the masticatory apparatus (Aristotle's lantern), which itself has five-fold radial symmetry. It is located at the base of the lower oral hemisphere of the sea urchin's body, juxtaposed to the substratum. Figure 1 is a photograph of a partially dissected Aristotle's lantern of *Paracentrotus lividus*, the species studied here. The teeth are held together by calcareous jaw plates (pyramids) which are connected to each other by transverse muscle fibres. Each tooth can be divided into three parts along its long axis: the mature chewing part which projects out of the calcareous plate towards the substrate, the mid-shaft which is attached to a calcareous plate, and the soft aboral growing zone (plumula) (Märkel 1970). Most sea urchins feed by scraping algae from hard rock surfaces. The five teeth move centripetally and simultaneously, and the chewing tip of each tooth is worn down continuously. The tooth is, however, continuously renewed by the growth of new tooth parts starting in the plumula (Hyman 1955). Thus at any given time a single tooth contains all the stages of growth.

The mature part of the tooth of *P. lividus* consists of three main zones with different structures and functions

* To whom correspondence should be addressed.

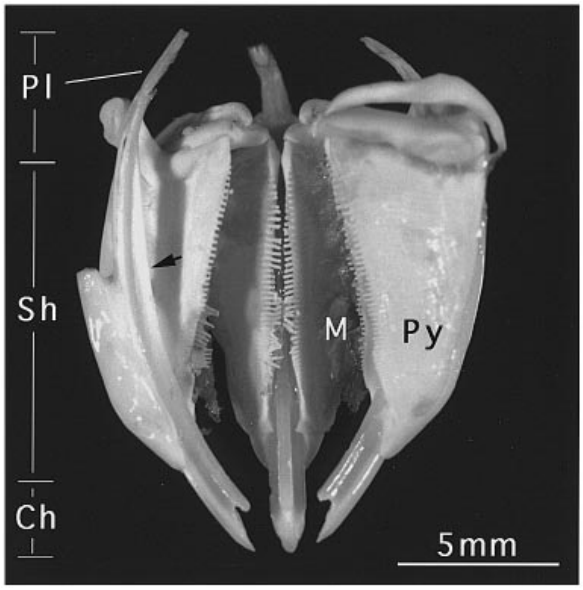

Figure 1. Optical photograph of a partially dissected Aristotle's lantern of *P. lividus*. Two teeth were removed together with their jaws, and three elongated teeth are visible. The arrow designates the site where the immature part was dissected from the rest of the tooth. Ch, chewing part; Sh, shaft; Pl, plumula; Py, pyramid (jaw plate); M, muscle.

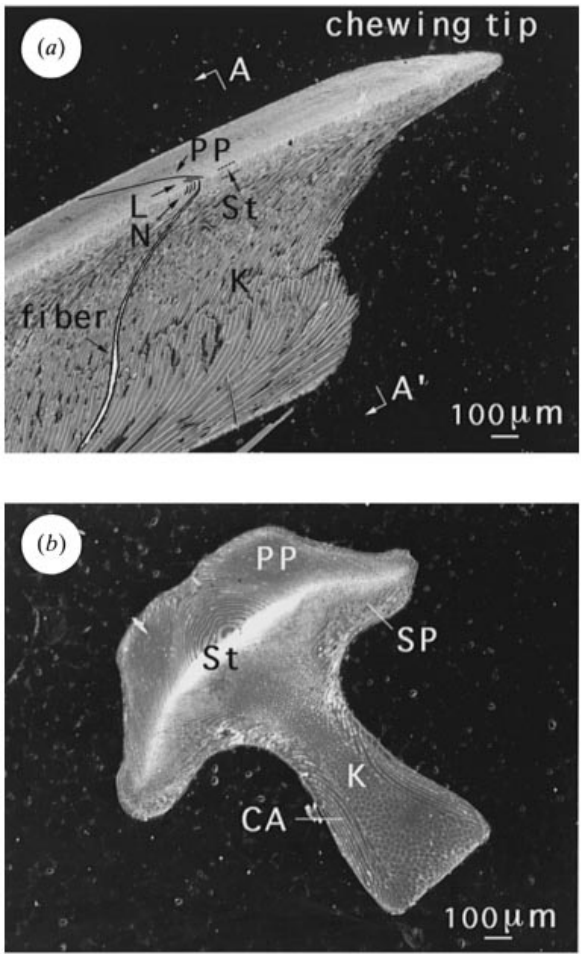

Figure 2. Longitudinal section (*a*) and cross-section (*b*) of the mature part of a sea urchin tooth. The section in (*b*) corresponds to A–A′ in (*a*). Polished samples were etched with 0.1 N HCl for 10 s. PP, primary plate zone; St, stone part; K, keel; SP, secondary plate; CA, carinar appendages of secondary plates; L, lamellae; N, needles.

(figure 2): the primary plate zone, the keel and the stone part. The latter is the main working part of the tooth and is also the hardest zone (Märkel & Gorny 1973). Each zone is composed of several basic structural elements. The primary plates are the main structural components of the layered portion of the primary plate zone. They are parallel to each other, but lie oblique to the long axis of the tooth shaft. The stone part contains calcareous needles, which are connected to the primary plates by small calcareous plates called lamellae. Prisms are the major components of the keel. Secondary plates and their carinar appendages form the outer layer of the keel. Once the basic structural elements are formed, the remaining spaces are filled by calcareous discs (Märkel 1970). Figure 2 shows the locations and orientations of these elements in the mature chewing part. The tooth also contains about 0.2–0.25 wt% organic macromolecules, most of which are proteins (Weiner 1985; Veis *et al*. 1986).

The development of sea urchin teeth has been extensively studied (Märkel 1970; Kniprath 1974; Chen & Lawrence 1986; Märkel *et al*. 1986). A brief synopsis of the major events occurring in the plumula follows. The first mineralized components to form are the individual primary plates. They are produced by syncytial odontoblasts in the plumula. While they grow laterally, lamellae and needles begin to form on the side of the primary plate closest to the boundary with the stone part (figure 2*a*). The lamellae grow along the primary plate surface, but the needles grow roughly perpendicular to the primary plate into the stone part. Here some of them stop growing, whereas others continue growing into prisms. We shall refer to the needles and prisms together as fibres. Shortly after lamellae and needles begin to form, secondary plates and their carinar appendages appear on the lateral sides of the primary plates. The calcareous discs form only during the second stage of mineralization. They connect the above tooth elements together to produce the mature tooth.

Several studies of the structure–composition–function relations of sea urchin teeth have been published. The primary plate zone has a laminated structure, which can resist the pressure stress on this zone of the tooth during scraping (Märkel *et al*. 1977). The keel and stone part of a sea urchin tooth was described as a fibre-reinforced composite with the calcitic prisms acting as reinforcing fibres, and the discs as matrix. This kind of structure can have high tensile strength and can withstand the tensile stress imposed on this zone of the tooth during scraping (Brear & Currey 1976; Märkel *et al*. 1977). Although the main mineral component is calcite, the microhardness of the stone part is more than twice that of pure calcite (Märkel & Gorny 1973). The magnesium carbonate content of the mineral in this part is as high as 43.5 mol% in *Lytechinus variegatus*. This is the highest value found among natural magnesium-bearing calcites and is referred to as protodolomite (Schroeder *et al*. 1969).

PHILOSOPHICAL TRANSACTIONS OF THE ROYAL SOCIETY B BIOLOGICAL SCIENCES

Many morphological studies indicate that there are complex structural design strategies in sea urchin teeth, many of which are still not understood. We focus our study on the fibres, discs and the plates in terms of their structure, morphology and chemical composition. We also study fracture, crack behaviour and microhardness of the tooth in an effort to understand aspects of tooth function better in relation to structure.

2. MATERIALS AND METHODS

Specimens of *P. lividus* were collected alive from the Mediterranean Sea. The teeth were extracted from the masticatory apparatus (Aristotle's lantern) and were either processed immediately (fresh teeth) or were frozen (frozen teeth) for later use.

Thirty fresh teeth were dissected into five portions: one portion included the more mature and consolidated part from just above the top of the calcareous jaw plate (arrow in figure 1) to the chewing tip. The remaining less mature part (mostly in the plumula) was dissected into four roughly equal parts, with the first being the region closest to the forming tip. After rinsing with double-distilled water for a few seconds, the five portions were immersed in 1% sodium hypochlorite solution on a rocking table for 30 min to remove the soft tissues. This also facilitates the separation of the structural elements of the plumula. The samples were collected by centrifugation (8160 g for 5 min) and were then washed for 5 min with double-distilled water three times. After drying in a lyophilizer, the structural elements were separated under a stereomicroscope using a fine needle. The primary plates were collected from the first two portions closest to the forming tip and the carinar appendages of the secondary plates were dissected from the secondary plates of the fourth portion. The needles were broken off the primary plates from the second portion. The mid-shafts of the fibres were broken off the primary plates from the third portion and the big mature ends of the fibres, from the fourth portion. Different parts of the mature portion of the tooth (figure 2*b*) were sampled by extracting small amounts of material from polished cross-sections.

Powder X-ray diffraction analyses were performed on a Rigaku D/max–RB diffractometer using CuKα radiation at 45 kV and 140 mA. The ground samples were mixed with KCl powder (as an internal standard) and were mounted on a germanium sample holder. The samples were first scanned in a continuous mode ($2\theta =$ 5–50°, scan speed 0.25° min^{-1}). The calcite {104} peaks were then scanned at higher resolution to obtain the lattice parameters ($2\theta =$ 28–31°, step size 0.004°, 6 s step^{-1}). Infrared spectra were collected on a MIDAC Fourier transform infrared (FTIR) spectrometer using a resolution of 1 cm^{-1}. Samples were dispersed in KBr pellets. For calcium and magnesium content measurements, samples were dissolved in 1 N HNO_3, and were then analysed with a Perkin-Elmer 5100 GFAAS atomic absorption spectrometer, assuming that calcium and magnesium are the only two major cations existing in the minerals (Chave 1952; Raup 1966).

The teeth microstructure and fracture behaviour were studied by three different methods. One set of fresh teeth were broken manually in a roughly transverse section to obtain fractured surfaces. A second set of both fresh and frozen teeth were embedded in methyl methacrylate (Buehler Ultra-Mount). They were then ground and mechanically polished using diamond paste (from 6 to 1 μm). The samples were etched either with 0.1 N HCl for 10 s or with double-distilled water for 2 to 48 h. The third set of frozen teeth were immersed in Karnovsky's fixative, containing 1% paraformaldehyde and 2% glutaraldehyde, for 60 min at room temperature. They were embedded and mechanically polished before being demineralized in a 0.2 M EDTA buffer solution containing 2% glutaraldehyde (pH 7.4) for 10 to 60 min. Samples were postfixed in sodium cacodylate-buffered 2% osmium tetraoxide (OsO_4) for 2 h. They were washed with 0.2 M sodium cacodylate buffer and double-distilled water, and then lyophilized. All three sets of samples were coated with gold and were observed under a Jeol 6400 scanning electron microscope (SEM) at an accelerating voltage of 15–25 kV.

Vickers microhardness of the mature teeth was measured on embedded and polished sections with a Leitz microhardness tester attached to a Leitz Metallux 3 optical microscope. Samples were loaded with 50 g for 10 s. The embedding and polishing methods were the same as those described above. Samples were kept wet during testing. The microindentations were also observed with the SEM.

3. RESULTS

(*a*) *Fibres*: *key structural elements*

The fracture morphology of the stone part shows that it is composed of a parallel array of fibres, each of which is separated by a fine-grained matrix (figure 3*a*). These fibres have been referred to as 'needles', and the crystals that constitute the matrix as 'discs' (Märkel 1970). Polished and EDTA-etched surfaces show that the discs consist of very small crystals (about 50–80 nm in size), and they surround each fibre (figure 3*b*, arrows). Figure 3*b* also shows etched holes within each fibre, indicating that the core of the fibre in the stone part is more soluble than its outer layer. Fixed and etched polished surfaces reveal that there is a very thin organic sheath surrounding each fibre (figure 3*c*). There appears to be a fairly large amount of organic material within the disc matrix. The keel is also composed of calcitic fibres (called prisms) and discs (figure 4*a*, *b*), but the fibres are much larger than in the stone part, and the proportion of the discs much smaller. A continuous thin organic sheath surrounds each fibre (figure 4*c*). The rod-like organic material between the calcitic fibres in figure 4*c* is most probably the cell channel described by Märkel *et al.* (1977).

We observed that the microstructure changes continuously from the stone part to the keel. In fact many of the needle-shaped fibres of the stone part represent the thin ends of continuous fibres, which progress all the way to the keel. This was observed by Märkel *et al.*

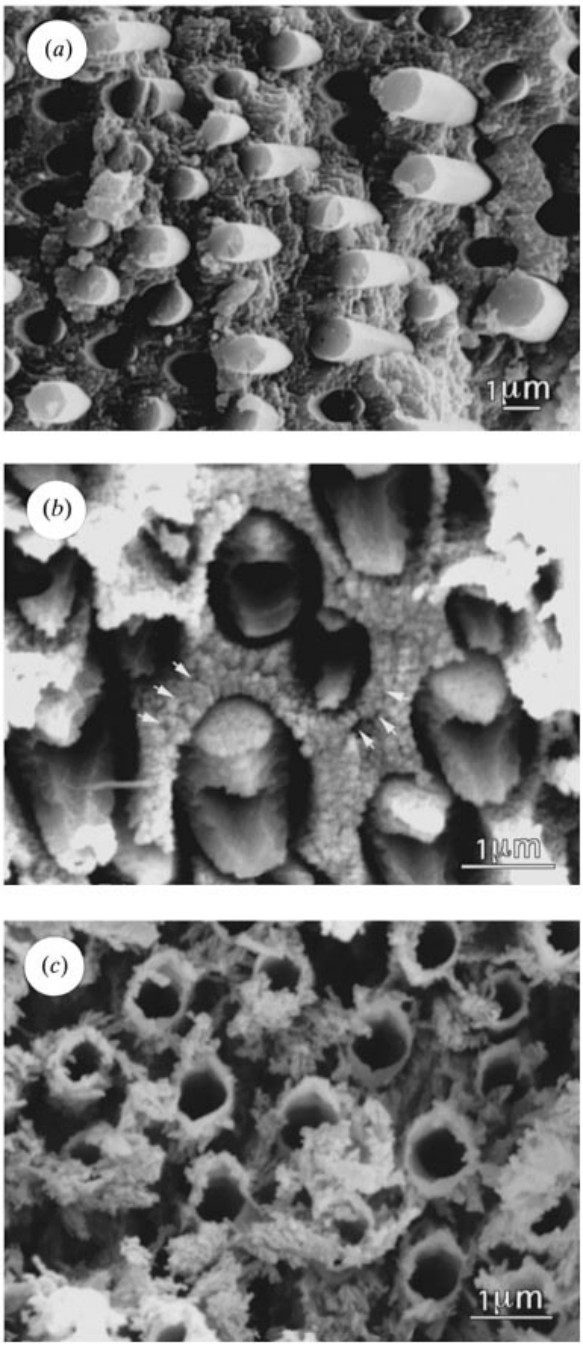

Figure 3. (*a*) Fracture morphology of the stone part showing its composite structure. (*b*) Polished and EDTA-etched surface of the stone part showing the polycrystalline discs (arrows) and the etched hole within each fibre. (*c*) Polished, fixed and EDTA-demineralized surface of the stone part showing the organic sheath surrounding each fibre.

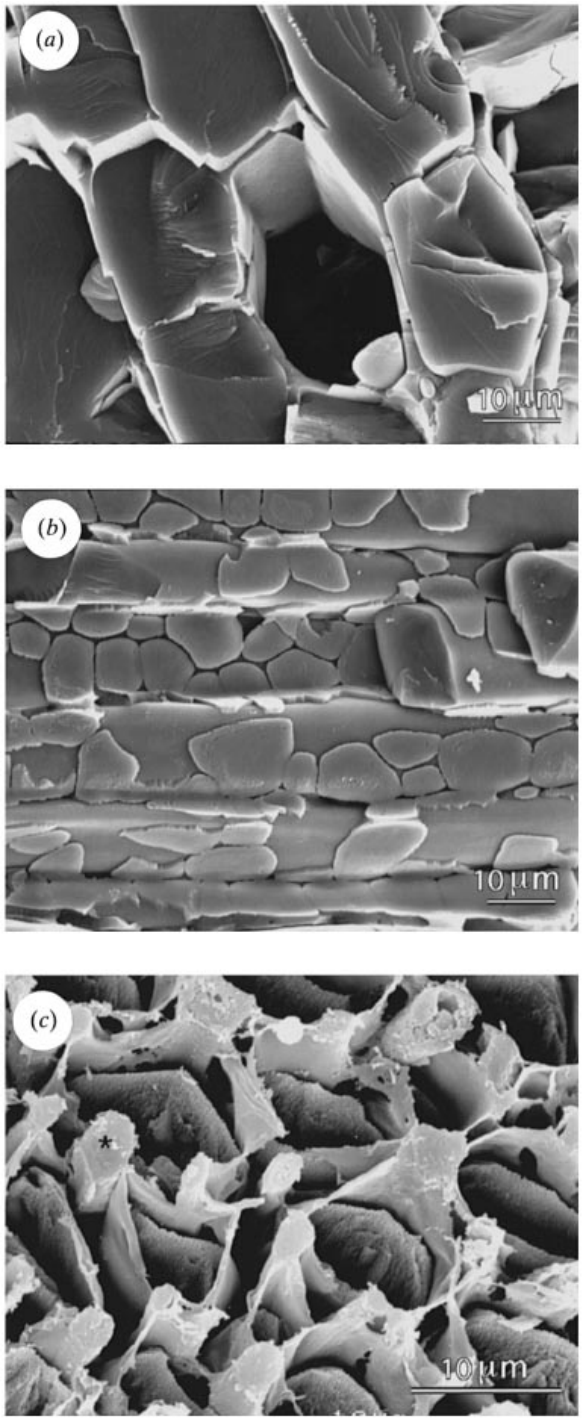

Figure 4. (*a*) Fracture morphology of the keel with the surface perpendicular to the fibres. (*b*) Fracture morphology of the keel with the surface parallel to the fibres revealing the discs. (*c*) Polished, fixed and EDTA-etched surface of a region midway from the stone part to the keel end, revealing organic sheaths and cell channels (asterisk).

(1970). Figure 5 shows an SEM micrograph of one such fibre, whose location and orientation are shown in figure 2*a*. There are three morphological characteristics of the fibres. They are S-shaped and parallel to each other along the tooth shaft (figure 5, figure 2*a*). The diameters of the fibres increase continuously and dramatically, from less than 1μm at the tip in the stone part (figure 3*a*) to about 20 μm at the shaft near the end of the keel (figure 4*a*). The shape of a fibre is round in the stone part and is polygonal in the keel. Because of the changes in fibre dimension, the volume fraction of fibres:discs changes continuously from about 50:50 in the stone part to about 90:10 at the end of the keel. Each fibre behaves like a single crystal of calcite in the polarizing microscope. This was confirmed by X-ray diffraction (Berman *et al.* 1993).

Some reports indicated that the magnesium contents change from place to place within the teeth (Schroeder *et al.* 1969). We therefore examined the possibility that the magnesium contents differ within a single fibre.

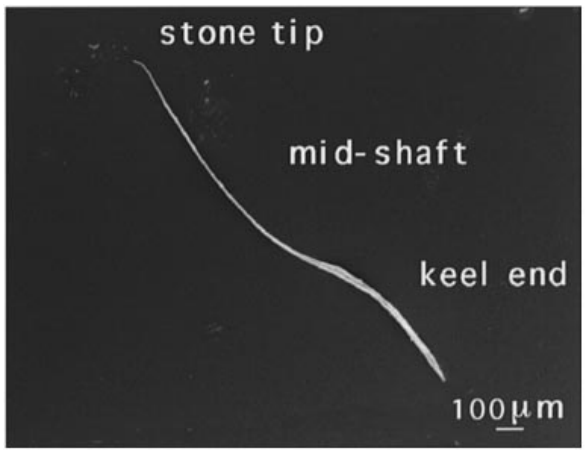

Figure 5. SEM micrograph of one isolated calcified fibre. Its position in the tooth is shown in figure 2*a*.

The tips (needles), mid-shafts and the large prismatic ends were dissected mechanically and analysed. FTIR spectra show no obvious changes in the three major absorption bands at around 1419, 1087 and 876 cm^{-1}. The in-plane deformation mode $\nu 4$ does, however, change from 717 cm^{-1} at the stone tip of the fibre to 714 cm^{-1} at the keel end. Note that $\nu 4$ for pure synthetic calcite is at 713 cm^{-1} and the total stone part has a broad peak at around 720 cm^{-1} (figure 6*a*). Powder X-ray diffraction (XRD) patterns of the {104} reflections are shown in figure 6*b*. There is clearly a shift in the 2θ value, corresponding to a change in *d*-spacing from 3.00 Å at the stone tip to 3.02 Å at the keel end. Both the FTIR and XRD results thus indicate that there is a systematic change of magnesium content along individual calcitic fibres. The deduced magnesium content of the stone tip, mid-shaft and prismatic end of the fibres is shown in table 1. An increase from about 4.5 mol% in the keel end to 13 mol% in the stone tip was observed. The same trend was obtained when samples were extracted from a cross-section through the stone part to the end of the keel close to the mature scraping surface and analysed with IR and XRD.

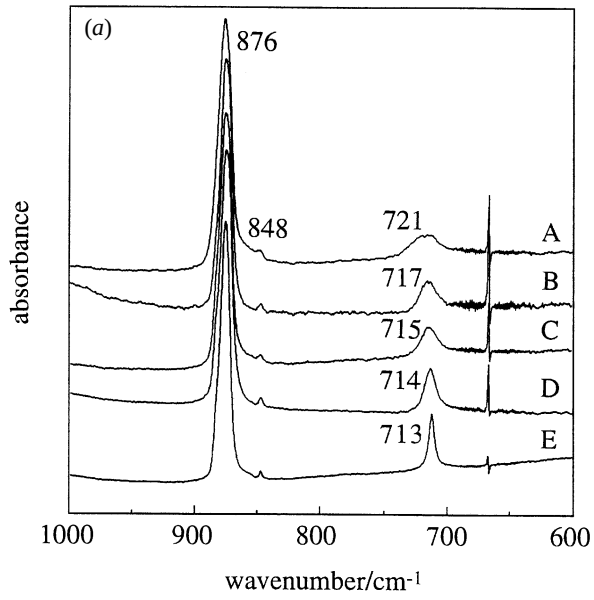

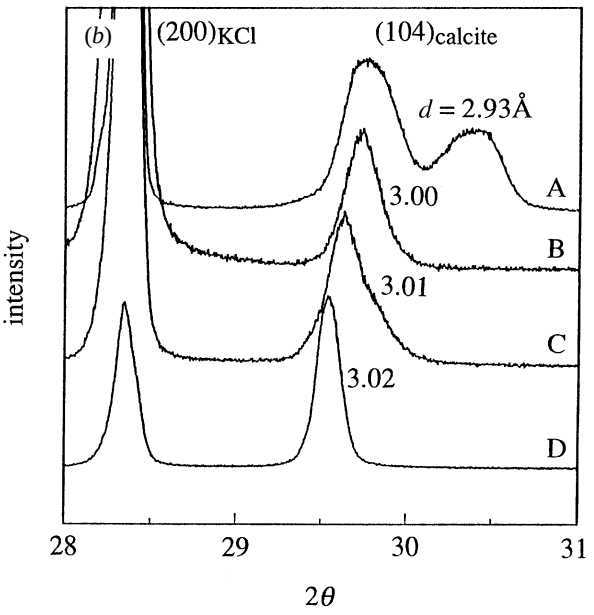

Figure 6. FTIR spectra (*a*) and X-ray powder diffraction patterns (*b*) of the stone part and different parts of fibres. A, total stone part; B, stone tips of fibres; C, mid-shafts of fibres; D, keel ends of fibres; E, pure synthetic calcite.

(*b*) *The discs: space fillers*

The discs filling the space between fibres are very small and adhere to the fibres. It is therefore very difficult to isolate them. The stone part was separated mechanically and its IR and XRD spectra are shown in figures 6*a* and *b*, respectively. The $\nu 4$ absorption band in the IR spectrum is composed of two overlapping peaks, one around 717 cm^{-1}, the other around 721 cm^{-1}. This implies the presence of two types of magnesium-bearing calcite minerals in the fibres and discs. We confirmed that two sets of diffraction peaks are present in the XRD spectrum: one at a position corresponding to that of the stone tip of the fibres, and the other at much higher 2θ values. The former corresponds to calcite with about 13 mol% $MgCO_3$, and the latter to 35 mol% $MgCO_3$. Back-scattering electron micrographs (not shown) of the transversely polished stone part show that the fibres are white, while the discs between the fibres are black. This indicates that the discs have a higher concentration of magnesium than the fibres. Therefore, the high magnesium diffraction peak originates from the discs.

The discs constitute about half (by volume) of the stone part. We previously measured the magnesium content of the other half, namely the fibre tips. An analysis of the total stone part could then provide an independent means of estimating the magnesium content of the discs. The magnesium content of the total stone part of *P. lividus* measured by atomic absorption spectrometry is 24 mol%, from which the magnesium carbonate content in the discs is calculated to be 35 mol%. In the stone part of *L. variegatus*, Schroeder found calcite with a magnesium content as high as 43.5 mol%, which he designated as proto-

Table 1. *Magnesium contents* ($MgCO_3$ mol %) *of sea urchin teeth*

	keel end of fibre	mid-shaft of fibre	stone tip of fibre	stone part	primary plate	carinar appendage
atomic absorption	4.7	10.0	14.1	24.0	8.4	4.8
X-ray diffraction	4.5	8.0	12.0	35.0	8.5	3.5

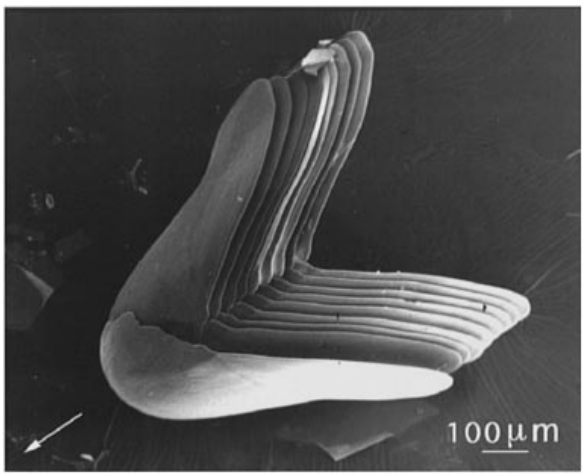

Figure 7. Aligned primary plates taken from the plumula of a tooth. The arrow indicates the direction of the chewing tip.

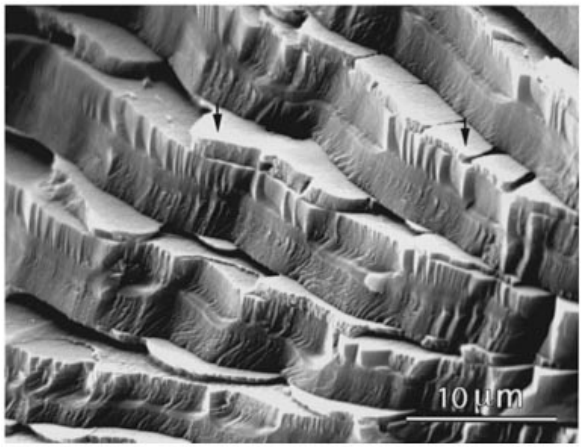

Figure 8. Fracture morphology of the primary plate part. The arrows indicate discs between primary plates. Crack steps are visible at the primary plate/disc interface and at the centre of each plate.

dolomite (Schroeder *et al*. 1969). In the case of *P. lividus* it is also probably protodolomite, as the XRD pattern is typical of calcite, without any detectable superstructure dolomite reflections.

(*c*) *The primary plate: a sandwich-like structure*

Stacks of aligned primary plates constitute the main structural component of this zone. Figure 7 shows primary plates from the forming part of the tooth. The thickness of each of the primary plates is about 1 µm near the stone part and increases to about 5 µm near the outer tooth surface. In the mature part of the tooth, the space between primary plates is filled with discs (figure 8, arrow). Their morphology is similar to the

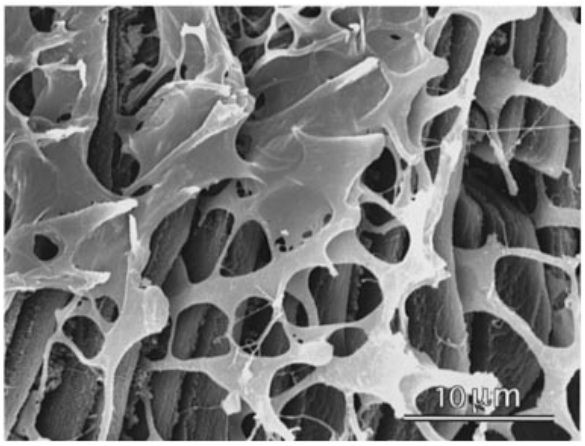

Figure 9. SEM photograph showing the organic sheaths at the primary plate/disc interface as well as the network-like cell channels in the disc layer. The sample was fixed and then decalcified with EDTA.

discs between the fibres in the keel (figure 4*b*). The empty spaces between the discs in figure 8 were occupied by cell channels, as was described by Märkel *et al*. (1977). These have a network morphology, that can be seen in teeth that were fixed and decalcified with EDTA (figure 9). A thin organic sheath is present between the primary plate and the layer of discs (figure 9).

Each primary plate behaves like a single calcite crystal in the polarizing microscope. The plate structure is however more complicated. The fractured cross-sectional surface of a primary plate clearly shows calcite cleavage steps, except for a thin central layer which is smooth (figure 10*a*). This implies that there is a structural difference between the outer layers and the central layer of each individual primary plate. When the polished primary plate was etched with 0.1 N HCl for 10 s or with double-distilled water for a few hours, a deep groove formed in the centre of each plate, indicating that the central layer is more soluble than its outer layer (figure 10*b*). A similar etching behaviour was previously described for the needles in the stone part (figure 3*b*). FTIR and XRD analyses (spectra not given here) showed that only one crystalline mineral is present, namely calcite. At this stage we can only infer that the central layer is amorphous calcium carbonate, as its solubility in water is much greater than that of calcite, and it fractures isotropically without preferential cleavage planes.

The $MgCO_3$ content of the primary plate is 8.4 mol % when measured by atomic absorption spectrometry, and 8.5 mol % based on the XRD {104} peak (table 1). Table 1 also shows the magnesium content of the carinar appendage of the secondary

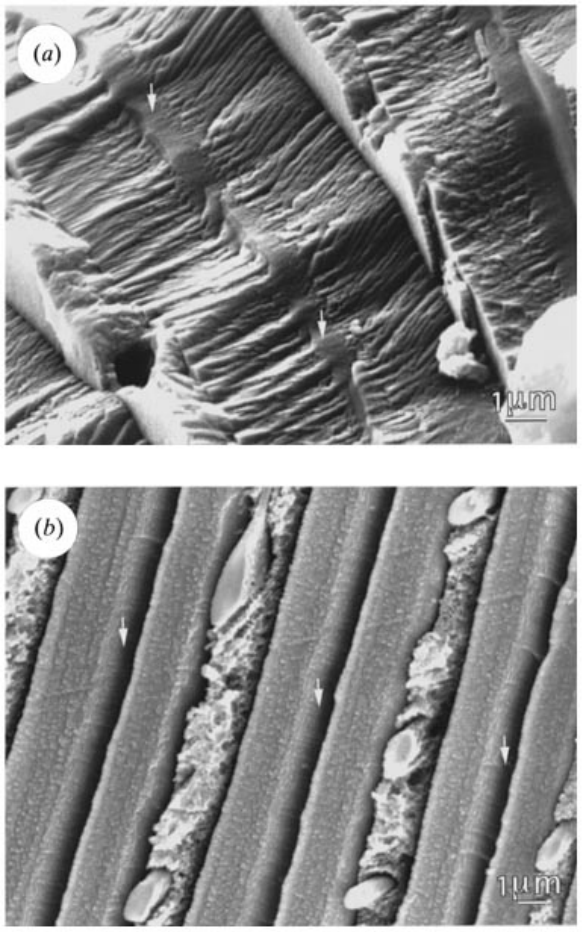

Figure 10. (*a*) Fracture morphology of primary plates showing cleavage steps on both sides of a primary plate and a smooth central layer (arrows). (*b*) Polished and 0.1 N HCl etched surface showing a deep groove (arrows) in the centre of each plate.

plate, which develops from the primary plate and constitutes the outer layer of the keel. Its magnesium carbonate content is 4.8 mol%. The magnesium content thus clearly changes within different parts of the plates.

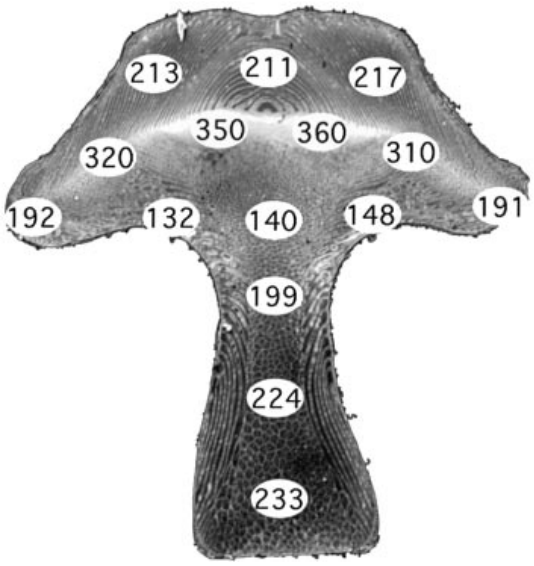

Figure 11. Vickers microhardness values (in kg mm^{-2}) on different zones of a tooth cross-section. The background is the same as figure 2*b*.

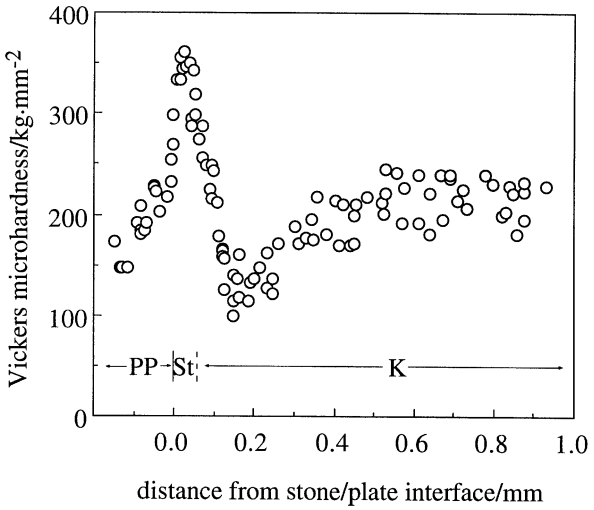

Figure 12. Vickers microhardness distribution on the longitudinal section of a tooth. The section plane is the same as figure 2*a*.

(*d*) *Microhardness, fracture and crack behaviour*

Hardness is an important mechanical property of all teeth. Variations in microhardness in different parts of the sea urchin tooth cross-section are shown in figure 11. The hardness of the stone part is much higher than that of the keel and the plate zone, and it decreases gradually from the central stone part to the two wings. The hardness reaches its lowest value (*ca.* 140 kg mm^{-2}) in the area between the stone part and the keel. Figure 12 shows the microhardness variations in a longitudinally sectioned tooth at the same location as shown in figure 2*a*. The hardness values were plotted against their distances from the primary plate/stone interface. Again, the hardness is highest in the stone part and sharply decreases in the plate zone. On the keel side, the microhardness drops to a sharp minimum, then rises to a plateau. Variations of hardness in different zones of the tooth were previously reported by Märkel & Gorny (1973) for *Sphaerechinus granularis*, although the absolute values are lower than those obtained here.

One of the main morphological features of a transversely fractured tooth is that the central stone part stands out sharply when viewed from the chewing tip side. Figure 13 is a typical SEM photograph of such a fractured surface. The central sharp tip is surrounded by both primary plates and the S-curved fibres. The topographic profile produced by manual fracture is very similar to the profile of the chewing tip shown in figure 2*a*, where the tooth was worn naturally during feeding. The natural tip profile follows the curved outline of fibres on the keel side and of the primary plates on the other side. Therefore, the sharp profile of the tooth has a close relation to the geometrical shape and arrangement of the main structural elements. We can also deduce from figure 13 that an important factor contributing to the sharp profile of the stone part is that the plate/disc interfaces and the fibre/disc interfaces are relatively weak, so that cracks can easily

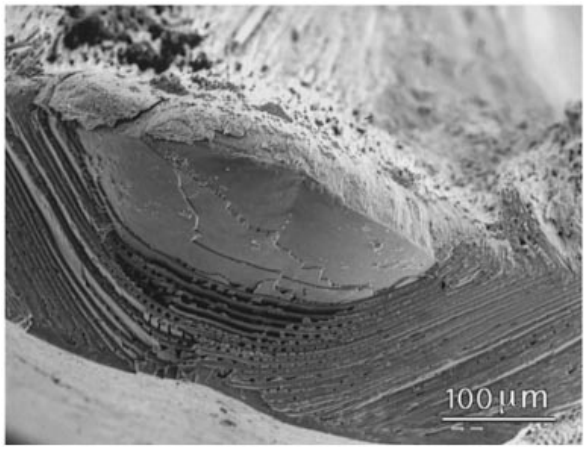

Figure 13. Fractured surface of a mature sea urchin tooth showing the sharp stone part standing out from the fracture.

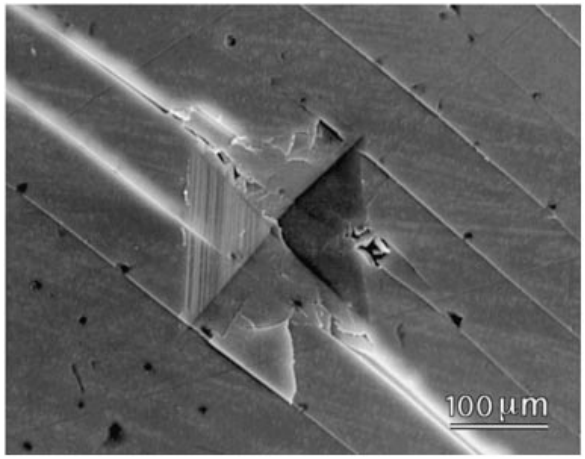

Figure 14. Parallel cracks along the primary plate/disc interfaces, induced by microindentation.

propagate along these interfaces with only minor deflections. Material is thus preferentially lost from around the stone part during feeding. The weakness of the plate/disc interface can be directly observed when a microindentation is made transverse to the primary plate (figure 14). Cracks preferentially occur at the plate/disc interfaces.

The fracture morphology profile from the stone part to the keel changes dramatically but continuously. The fracture surface of the stone part (figure 3*a*) is morphologically quite similar to the fracture surface of a synthetic fibre-reinforced matrix composite. Many fibres stand out of the main crack plane of the matrix surrounding the fibres, while many others were pulled out of the fracture surface, leaving holes. In the keel, fibre pullout also occurs during fracture, but due to the increase in the fibre dimensions and the decrease in the numbers of fibres, the cleavage fracture of the large fibres themselves gradually becomes the feature that dominates the fracture surface (figure 4*a*). Figure 15 shows a microindentation from the stone part, one from midway between the stone part and the keel, and one at the end of the keel. Under the same load, only very short cracks appear at the four corners of the indentation in the stone part, while at the keel, many cracks, some of them fairly long, can be seen around

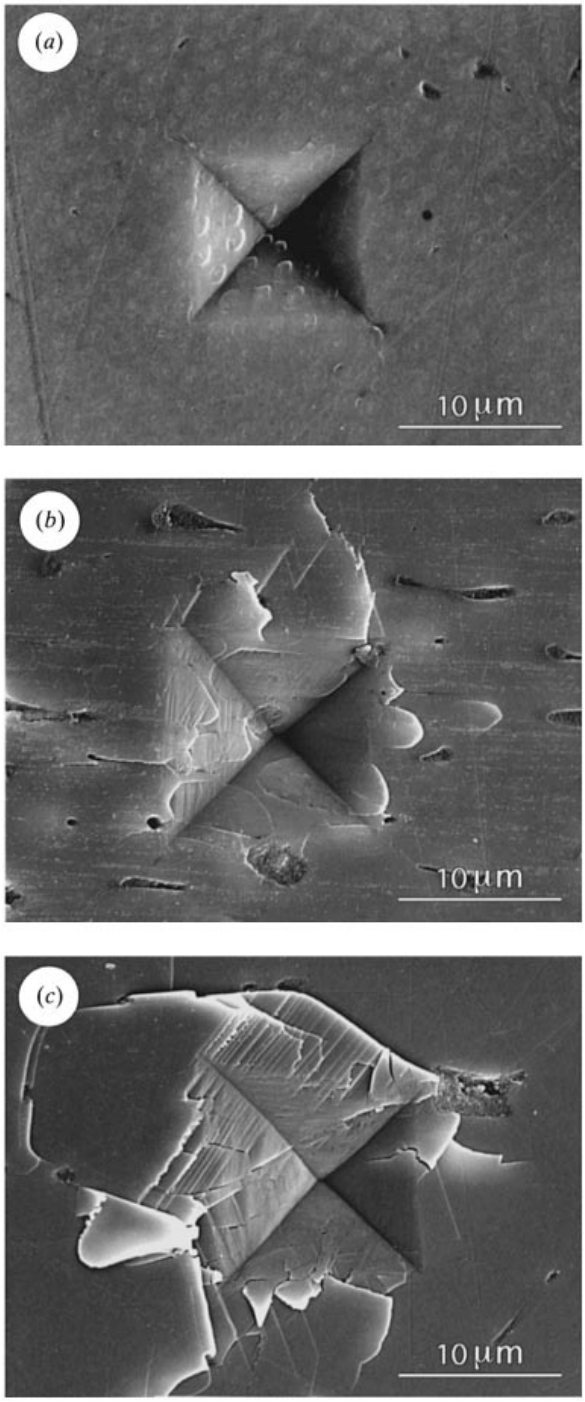

Figure 15. Microcracks induced by microindentations. (*a*) Stone part. (*b*) Midway from the stone part to the keel. (*c*) End of the keel.

the indentation. The resistance to cracking, and therefore the fracture toughness, is highest in the stone part, and lowest at the end of the keel.

4. DISCUSSION

The structure, morphology and chemical composition of whole areas and isolated components of sea urchin teeth have been studied to understand better the structure–function relations in this advanced biogenic composite material. In particular we show that the long fibres that progress from the stone part to

PHILOSOPHICAL TRANSACTIONS OF THE ROYAL SOCIETY B BIOLOGICAL SCIENCES

the keel of the tooth dramatically change their shape, size and magnesium content along their length. We also show that the discs in the stone part of *P. lividus* have a very high magnesium content, comparable to that observed for *L. variegatus*. The primary plates have a very unusual sandwich-like structure, with a calcitic envelope surrounding a thin, apparently amorphous $CaCO_3$ layer. The variations in microhardness, fracture and crack behaviour provide more insight into the structure–function design features of the tooth.

(*a*) *Unique fibre-reinforced ceramic matrix composite*

The main structural element in the stone part and the keel of sea urchin teeth consists of calcitic fibres. Between the fibres are intercalated high magnesium calcite discs. There are small amounts of organic material present between the fibres and the discs. This part of the tooth can, therefore, be considered as a kind of fibre-reinforced ceramic matrix composite. Note that the organic material is also usually referred to as 'matrix' according to its function in the regulation of mineral growth in biomineralization (Lowenstam & Weiner 1989). Here we refer to the calcitic discs as 'matrix', following the composite materials terminology.

The stone part of sea urchin teeth has been described as a fibre-reinforced composite (Brear & Currey 1976; Märkel *et al.* 1977). We determined that the magnesium content of the reinforcing fibres decreases from about 13 mol% in the stone tip to about 4.5 mol% in the keel end. We also found that the diameter of the reinforcing fibres increases from less than 1 μm in the stone part to about 20 μm at the end of the keel. As a result, the volume fraction of fibres : discs of the resulting fibre-reinforced composite changes gradually from about 50:50 to 90:10. This is therefore a gradient material. The gradient structure and composition are related directly to the variations in mechanical properties, i.e. microhardness, fracture morphology and toughness. These in turn meet the needs of the special self-sharpening function of the teeth (see below).

The hardness gradient of the teeth shown in figures 11 and 12 may be attributed to variations both in structure and composition. The atomic radius of magnesium is smaller than that of calcium. The occlusion of magnesium into the calcite crystal lattice causes lattice distortion, which in turn increases the sliding resistance of dislocations and the deformation resistance of the crystals. The discs, which are composed of high magnesium calcite, are consequently expected to have a higher lattice distortion and to be harder than the low magnesium calcite of the fibres. Analogously, the small tips of the fibres with a relatively high magnesium content will be harder than their large ends. The stone part, which is composed of the small tips of the fibres and large amount of discs, will thus be harder than the keel part, which is mainly composed of the large extremities of fibres. The hardness minimum in the keel (figures 11 and 12) is most probably due to the coarse and soft cell channels present in this area (figure 4*c*).

The change in the fracture morphologies and the decrease in toughness from the stone part to the keel (figures 3*a*, 4*a* and 15) are closely related to the gradual increase in fibre dimensions. The fracture surface of the stone part as well as of the keel (figures 3*a* and 4*a*) has a typical fibre pullout morphology, although the cleavage of the fibres themselves is the dominant feature in the keel. Fibre pullout in composites occurs in steps (Harris 1980; Marshall & Evans 1985; Thouless & Evans 1988). In the first step, the fibre/matrix interface is debonded under stress, with the energy stored in the strained fibres. The fibre is then broken some distance away from the main crack plane. This process causes the crack to deflect at the fibre/matrix interface. In the last step, the broken fibre is pulled out of the matrix, with the work being done against friction. All these steps increase the crack propagation resistance, and consequently the fracture toughness of the material. Furthermore, the toughness increases with increasing area of the fibre/disc interface. Indeed, in the stone part of sea urchin teeth the fibre/disc interfacial area is calculated to be as high as 2×10^6 m^2 per cubic metre, while at the end of the keel the interfacial area is only 0.2×10^6 m^2 per cubic metre. The toughness gradient from the stone part to the keel (figure 15) can thus be rationalized.

Fibre-reinforced composites are very common in the field of synthetic materials. In order to optimize the strength and toughness of these composites, one of the major problems to be solved is how to design the interface structure so as to obtain a moderate interfacial strength between fibres and matrix (Marshall & Evans 1985; Thouless & Evans 1988). Too strong an interface will inhibit fibre pullout, and thus decrease the toughness, while too weak an interface will damage the strength of the material. In the case of sea urchin teeth, the fibre pullout morphology and the superior toughness in the stone part clearly imply that the fibre/disc interface is well controlled. Each fibre is surrounded by a thin organic sheath (figures 3*c* and 4*c*), and debonding probably occurs at the interface between the fibres and the surrounding sheath. This thin organic layer most probably plays a key role in optimizing the interfacial strength between plates and discs. In the plumula, it has been found that each calcareous element is surrounded by an organic sheath (Kniprath 1974; Chen & Lawrence 1986; Märkel *et al.* 1986; Veis *et al.* 1986; Märkel *et al.* 1989). Here we found that the organic sheath persists in the mature stage of the tooth and may have an important contribution to the mechanical properties of the tooth. Further study is needed in order to elucidate the chemical and physical nature of this interfacial zone.

From the above analysis, we deduce that the material composing the stone part and the keel of sea urchin teeth is a unique kind of fibre-reinforced ceramic matrix composite, with a gradient in both microstructure and mechanical properties from one side to the other. The fibre/disc interface is also well designed and controlled. A deeper understanding of such structural design principles and their functions may provide useful information for the fabrication of advanced synthetic composites.

(*b*) *Laminated ceramic composite—the plates/discs complex*

The primary plate part of the sea urchin tooth has a sandwich-like or laminated structure formed of primary plates alternating with discs. As only a small amount of organic material exists between calcitic discs and plates, this part of the tooth can be regarded as a laminated ceramic composite.

The fracture surface of the primary plate zone is usually stepped. Cracks were observed to stop or be deflected at the plate/disc interface (figure 8). Such crack deflection will significantly increase the toughness of this part, due to blunting of the crack tip and an increased energy of fracture (Cook & Gordon 1964). The use of layered structures to increase toughness is quite common in synthetic ceramic composites and has also been observed in biological materials such as the nacreous layer of mollusc shells (Currey 1977; Jackson *et al*. 1988). In order to take advantage of the crack deflection toughening mechanism, the plate/disc interfacial strength should also be well controlled. Again, we emphasize the important role of the organic sheath separating the plates and the discs in optimizing the interfacial strength. Obviously, the mechanical properties (toughness, strength, etc.) of the laminated structure in this part are optimal when the main crack propagates perpendicular to the interface plane. They are much weaker when the main crack propagates parallel to the plate/disc interface. This kind of anisotropy in mechanical behaviour has a direct relation with the self-sharpening of the teeth (see below).

A remarkable observation is the fracture behaviour within each primary plate. There are two distinct fracture morphologies within each individual primary plate: the non-structured smooth fracture surface of the central layer, which is probably composed of amorphous $CaCO_3$, and the cleavage fracture morphology of the outer calcitic layer (figures 8 and 10*a*). There are clear crack steps in the area between the central layer and the outer crystalline layer, indicating that the crack was also blunted and deflected within primary plates. The main reason for the crack deflection here is most probably the structural discontinuity within the plate rather than a weak interface. The crack propagates easily along the cleavage planes of the outer calcitic layer of the plate, and is deflected when it meets the central amorphous layer, offering resistance to further propagation of the crack. The toughness of the whole laminated material is thus further increased.

In the study of the teeth of *Eucidaris tribuloides*, Märkel reported 'a central non-calcified cleft' on the fractured primary plates treated with ultrasound (Märkel 1990). It would appear from our study that this central cleft was most probably filled with amorphous $CaCO_3$ which was preferentially etched during ultrasonic cleaning. The coexistence of amorphous and crystalline minerals has been observed in several biological systems, such as sea urchin larval spicules (Beniash *et al*. 1997), and the spicules from the calcareous sponge *Clathrina contorta* (Aizenberg *et al*. 1996). The structural discontinuity presumably has mechanical functions also in these biological materials. The above basic concepts of increasing toughness by combining materials with different structures, in addition to using a laminated structure, may also have application to materials science.

(*c*) *Biological structure–function relations: self-sharpening*

Although the five sea urchin teeth are worn continuously during feeding, their chewing tips are always sharp. This phenomenon of self-sharpening and its relations to structure are of great interest to both materials scientists and biologists. A detailed study of the self-sharpening mechanisms may provide some useful information for the structural and material design of cutting tools, as well as a deeper understanding of the functions of biological structures. The self-sharpening of sea urchin teeth appears to result from the combination of careful control over the compositions and morphologies of its structural elements, as well as of the design of the interfaces between them, as detailed below.

(i) *The shapes of key structural elements*

The outline of the primary plate side of the sharp chewing tip follows the slightly curved surface of the primary plates (figures 2*a* and 7), while the worn surface of the stone part and the keel follows the path of the S-shaped fibres (figures 2*a* and 5). The sharp profile of the chewing tip thus has a direct relation with the geometrical shape of the main structural elements and their spatial arrangement.

(ii) *The interfaces*

An additional requirement for self-sharpening is that the interfaces of plate/disc and fibre/disc should be relatively weak. This will allow the cracks introduced during feeding to propagate more easily along these interfaces rather than perpendicular to them. Preferential cracking is indeed observed to occur along the primary plate/disc and fibre/disc interfaces (figures 3*a*, 8, 13 and 14). A well-controlled interface plays a key role in the self-sharpening mechanism of the tooth, in addition to its important contributions to the toughness.

(iii) *Tailoring the hardness*

As a chewing tool, the hardness of a tooth should be high enough to prevent rapid wear during feeding. On the other hand, if the hardness of the sea urchin tooth were uniform, it would not be self-sharpening. Therefore, a controlled distribution of hardness in different parts of the tooth is necessary. The stone part in fact has the greatest hardness, and it decreases gradually towards the primary plate part and the keel. This hardness gradient ensures that the hard stone part will be worn down more slowly than the surrounding area, and will stand out during feeding. The microstructure and compositions in sea urchin teeth have thus been carefully tailored to achieve a gradient in hardness,

which also contributes to the self-sharpening mechanisms.

It is of interest to compare the structure–function relations of sea urchin teeth with those of other teeth. Usually, a tooth can be roughly divided into two main parts with different functions: the working part which is hard and therefore wear-resistant, and the softer supporting part which can withstand the possible impacting, compressive or tensile stresses imposed on it. In sea urchin teeth, all the parts are composed of the same mineral (calcite), with more or less the same volume content. Differences in hardness and other mechanical properties between different zones are achieved mainly by changing the magnesium content, the size and morphology of calcite crystals. Mammalian teeth are also composed of only one mineral (carbonated apatite), but the hardness difference is mainly achieved by the change of mineral content in different parts. The hard enamel layer consists of about 97 wt % carbonated apatite, while the mineral content of the inner softer crown dentine is only about 69 wt % (Waters 1980). Contrary to the strategies used above, the radular teeth of some chitons (Polyplacophora) and limpets (Gastropoda) in the mollusc phylum introduce several minerals with varying hardness values to achieve the differences in hardness. The mature radular teeth of common Chitonida are composed of hard magnetite on the working tooth margin and the entire posterior region, and consist mainly of carbonate apatite in the central core and most of the anterior tooth surface (Lowenstam 1967; Lowenstam & Weiner 1985, 1989). The radular teeth of limpets is rich in goethite at the hard-working posterior side of the cusp, and contains mainly opal in the lower part of the anterior side of the cusp (Lowenstam 1962, 1971; Mann *et al*. 1986; Van der Wal 1989).

Some types of teeth discussed above are self-sharpening. The incisors of rodents are worn away at the working tip, and are continuously renewed at the growing end. During feeding, the softer dentine is eroded faster than the hard enamel which overlies the dentine on the labial side of the tooth. Thus the working tip is always sharper on the hard enamel side (Currey 1990). It is not known whether the structure of the crown dentine itself contributes in some way to self-sharpening. In limpets, the acicular crystals in the anterior region are preferentially aligned, their orientation being coincident with the wear surface. This oriented internal structure is thus believed to have the function of sharpening the teeth (Van der Wal 1989). In sea urchin teeth, both strategies of introducing a hardness gradient and arranging the internal structure are present.

There are many structure–function design strategies used in teeth, some of them shared by different kinds of teeth, while others are specific to certain species and are adapted to their special living circumstances and biological functions. The study of sea urchin teeth in this paper has elucidated some of these strategies. Teeth therefore offer unique opportunities to elucidate novel structure–function relations in biological materials.

We thank Professor H. D. Wagner for comments, J. Aizenberg and Y. Freedman for atomic absorption measurements, and E. Beniash for his assistance in some SEM experiments. This study was supported by a US Public Health Service grant (DE06954) from the National Institute of Dental Research, NIH. S.W. is incumbent of the I. W. Abel Professorial Chair of Structural Biology, and L.A. is incumbent of the Patrick E. Gorman Professorial Chair of Biological Ultrastructure.

REFERENCES

Addadi, L. & Weiner, S. 1992 Control and design principles in biological mineralization. *Angew. Chem., Int. Ed. Engl.* **31**, 153–169.

Aizenberg, J., Lambert, G., Addadi, L. & Weiner, S. 1996 Stabilization of amorphous calcium carbonate by specialized macromolecules in biological and synthetic precipitates. *Adv. Mater.* **8**, 222–226.

Barnes, R. D. 1987 *Invertebrate zoology*. Philadelphia: CBS College Publishing.

Beniash, E., Aizenberg, J., Addadi, L. & Weiner, S. 1997 Amorphous calcium carbonate transforms into calcite during sea urchin larval spicule growth. *Proc. R. Soc. Lond.* B. **264**, 461–465.

Berman, A., Hanson, J., Leiserowitz, L., Koetzle, T. F., Weiner, S. & Addadi, L. 1993 Biological control of crystal texture: a widespread strategy for adapting crystal properties to function. *Science, Wash.* **259**, 776–779.

Brear, K. & Currey, J. D. 1976 Structure of a sea urchin tooth. *J. Mater. Sci. Lett.* **11**, 1977–1978.

Chave, K. E. 1952 A solid solution between calcite and dolomite. *J. Geol.* **60**, 190–192.

Chen, C.-P. & Lawrence, J. M. 1986 The ultrastructure of the plumula of the tooth of *Lytechinus variegatus*. *Acta Zool.* **67**, 33–41.

Cook, J. & Gordon, J. E. 1964 A mechanism for the control of crack propagation in all-brittle systems. *Proc. R. Soc. Lond.* A **282**, 508–520.

Currey, J. D. 1977 Mechanical properties of mother of pearl in tension. *Proc. R. Soc. Lond.* B **196**, 443–463.

Currey, J. D. 1990 Biomechanics of mineralized skeletons. In *Skeletal biomineralization: patterns, processes and evolutionary trends*, vol. 1 (ed. J. G. Carter), pp. 11–25. New York: Van Nostrand Reinhold.

Harris, B. 1980 The mechanical behaviour of composite materials. In *Symposia of the Society for Experimental Biology 34*. (*The mechanical properties of biological materials*), (ed. J. F. V. Vincent & J. D. Currey), pp. 37–74. Cambridge University Press.

Heuer, A. H., Fink, D. J., Laraia, V. J. *et al*. 1992 Innovative materials processing strategies—a biomimetic approach. *Science, Wash.* **255**, 1098–1105.

Hyman, L. H. 1955 *The invertebrates. IV. Echinodermata*. New York: McGraw–Hill.

Jackson, A. P., Vincent, J. F. V. & Turner, R. M. 1988 The mechanical design of nacre. *Proc. R. Soc. Lond.* B **234**, 415–440.

Kniprath, E. 1974 Ultrastructure and growth of the sea urchin tooth. *Calc. Tiss. Res.* **14**, 211–228.

Lowenstam, H. A. 1962 Goethite in radular teeth of recent marine gastropods. *Science, Wash.* **137**, 279–280.

Lowenstam, H. A. 1967 Lepidocrocite, an apatite mineral, and magnetite in teeth of chitons (Polyplacophora). *Science, Wash.* **156**, 1373–1375.

Lowenstam, H. A. 1971 Opal precipitation by marine gastropods (Mollusca). *Science, Wash.* **171**, 487–490.

Lowenstam, H. A. & Weiner, S. 1985 Transformation of amorphous calcium phosphate to crystalline dahllite in the radular teeth of chitons. *Science, Wash.* **227**, 51–53.

Lowenstam, H. A. & Weiner, S. 1989 *On biomineralization*. New York: Oxford University Press.

Mann, S., Perry, C. C., Webb, J., Luke, B. & Williams, R. J. P. 1986 Structure, morphology, composition and organization of biogenic minerals in limpet teeth. *Proc. R. Soc. Lond.* B **227**, 179–190.

Mann, S., Webb, J. & Williams, R. J. P. 1989 *Biomineralization, chemical and biochemical perspectives*. Weinheim: VCH Verlagsgesellschaft.

Märkel, K. 1970 The tooth skeleton of *Echinometra mathaei* (Blainville) (Echinodermata, Echinoidea). *Annotationes Zoologicae Japonenses*. **43**, 188–199.

Märkel, K. 1990 Biomineralization in echinoderms. In *Echinoderm research* (ed. C. De Ridder, P. Dubois, M.-C. Lahaye & M. Jangoux), pp. 277–282. Rotterdam: A. A. Balkema.

Märkel, K. & Gorny, P. 1973 Zur funktionellen anatomie der seeigelzähne (Echinodermata, Echinoidea). *Z. Morph. Tiere* **75**, 223–242.

Märkel, K., Gorny, P. & Abraham, K. 1977 Microarchitecture of sea urchin teeth. *Fortschr. Zool.* **24**, 103–114.

Märkel, K., Röser, U., Mackenstedt, U. & Klostermann, M. 1986 Ultrastructure investigation of matrix-mediated biomineralization in echinoids (Echinodermata, Echinoida). *Zoomorphology* **106**, 232–243.

Märkel, K., Röser, U. & Stauber, M. 1989 On the ultrastructure and the supposed function of the mineralizing matrix coat of sea urchins (Echinodermata, Echinoidea). *Zoomorphology* **109**, 79–87.

Marshall, D. B. & Evans, A. G. 1985 Failure mechanisms in ceramic-fiber/ceramic-matrix composites. *J. Am. Ceram. Soc.* **68**, 225–231.

Raup, D. M. 1966 The endoskeleton. In *Physiology of echinodermata* (ed. R. A. Boolootian), pp. 379–395. New York: Wiley Interscience.

Schroeder, J. H., Dwornik, E. J. & Papike, J. J. 1969 Primary protodolomite in echinoid skeletons. *Bull. Geol. Soc. Am.* **80**, 1613–1616.

Thouless, M. D. & Evans, A. G. 1988 Effects of pullout on the mechanical properties of ceramic matrix composites. *Acta Metall.* **36**, 517–522.

Van der Wal, P. 1989 Structural and material design of mature mineralized radula teeth of *Patella vulgata* (Gastropoda). *J. Ultrastruct. Mol. Struct. Res.* **102**, 147–161.

Veis, D. J., Albinger, T. M., Clohisy, J., Rahima, M., Sabsay, B. & Veis, A. 1986 Matrix proteins of the teeth of the sea urchin *Lytechinus variegatus*. *J. Exp. Zool.* **240**, 35–46.

Vincent, J. F. V. 1990 *Structural biomaterials*. Princeton University Press.

Waters, N. E. 1980 Some mechanical and physical properties of teeth. In *Symposia of the Society for Experimental Biology 34*. (*The mechanical properties of biological materials*), (ed. J. F. V. Vincent & J. D. Currey), pp. 99–135. London: Cambridge University Press.

Weiner, S. 1985 Organic matrix-like macromolecules associated with the mineral phase of sea urchin skeletal plates and teeth. *J. Exp. Zool.* **234**, 7–15.

Weiner, S. 1986 Organization of extracellularly mineralized tissues: a comparative study of biological crystal growth. *CRC Crit. Rev. Biochem.* **20**, 365–408.

Received 3 September 1996; accepted 14 November 1996

PHILOSOPHICAL TRANSACTIONS OF THE ROYAL SOCIETY B BIOLOGICAL SCIENCES